

The lysophosphatidic acid receptor LPA₁ links pulmonary fibrosis to lung injury by mediating fibroblast recruitment and vascular leak

Andrew M Tager^{1,2}, Peter LaCamera^{1,2,9}, Barry S Shea^{1,2,9}, Gabriele S Campanella¹, Moisés Selman³, Zhenwen Zhao⁴, Vasiliy Polosukhin⁵, John Wain^{1,6}, Banu A Karimi-Shah^{1,2}, Nancy D Kim¹, William K Hart¹, Annie Pardo⁷, Timothy S Blackwell⁵, Yan Xu⁴, Jerold Chun⁸ & Andrew D Luster¹

Aberrant wound-healing responses to injury have been implicated in the development of pulmonary fibrosis, but the mediators directing these pathologic responses have yet to be fully identified. We show that lysophosphatidic acid levels increase in bronchoalveolar lavage fluid following lung injury in the bleomycin model of pulmonary fibrosis, and that mice lacking one of its receptors, LPA₁, are markedly protected from fibrosis and mortality in this model. The absence of LPA₁ led to reduced fibroblast recruitment and vascular leak, two responses that may be excessive when injury leads to fibrosis rather than to repair, whereas leukocyte recruitment was preserved during the first week after injury. In persons with idiopathic pulmonary fibrosis, lysophosphatidic acid levels in bronchoalveolar lavage fluid were also increased, and inhibition of LPA₁ markedly reduced fibroblast responses to the chemotactic activity of this fluid. LPA₁ therefore represents a new therapeutic target for diseases in which aberrant responses to injury contribute to fibrosis, such as idiopathic pulmonary fibrosis.

Tissue injury initiates a complex series of host wound-healing responses. If successful, these responses restore normal tissue structure and function. If not, these responses can lead to tissue fibrosis and loss of function. In the lung, aberrant wound-healing responses to injury are thought to contribute to the pathogenesis of idiopathic pulmonary fibrosis (IPF)¹. IPF and other fibrotic lung diseases are associated with high morbidity and mortality, and are generally refractory to currently available pharmacological therapies. Better identification of the mediators linking lung injury and pulmonary fibrosis is needed to recognize new therapeutic targets for these diseases.

After cutaneous injury, fibroblasts migrate into the provisional fibrin matrix of the wound clot during granulation tissue formation². In IPF, fibroblasts analogously migrate into the fibrin-rich exudates that develop in the airspaces after lung injury³. Fibroblast chemoattractant activity is generated in the airspaces in IPF, and its extent correlates with disease severity⁴. A pathogenic role for fibroblast migration in IPF is further supported by the recent description of an accelerated variant of IPF⁵. Genes related to cell migration were upregulated in the lungs of these ‘rapid’ progressors, and their bronchoalveolar lavage (BAL) fluid induced significantly greater

fibroblast migration than BAL from ‘slow’ progressors⁵. We and others have reported evidence that inhibition of fibroblast migration can attenuate pulmonary fibrosis^{6–8}.

To identify the chemoattractant(s) mediating fibroblast migration in the injured lung, we biophysically characterized the fibroblast chemoattractant activity present in the airspaces in the bleomycin mouse model of pulmonary fibrosis. We show that fibroblast migration in this model is mediated by lysophosphatidic acid (LPA), acting through one of its specific G protein-coupled receptors (GPCRs), LPA₁. To evaluate the contribution of the LPA-LPA₁ pathway to pulmonary fibrosis *in vivo*, we then challenged LPA₁-deficient mice with bleomycin and found that they were markedly protected. Consistent with LPA contributing to fibroblast recruitment induced by lung injury, the accumulation of fibroblasts after bleomycin challenge was markedly attenuated in LPA₁-deficient mice. LPA also induces endothelial cell barrier dysfunction and vascular leak^{9,10}. Vascular permeability is increased throughout the early phases of repair after tissue injury¹¹ and may contribute to fibrosis¹². Consistent with LPA contributing to vascular leak induced by lung injury, we found that the vascular leak induced by bleomycin challenge was also markedly attenuated in LPA₁-deficient mice.

¹Center for Immunology and Inflammatory Diseases, Division of Rheumatology, Allergy and Immunology, and ²Pulmonary and Critical Care Unit, Massachusetts General Hospital, Harvard Medical School, CNY149-8301, 149 13th Street, Charlestown, Massachusetts 02129 USA. ³Instituto Nacional de Enfermedades Respiratorias, Mexico City, Mexico. ⁴Department of Obstetrics and Gynecology, Indiana University School of Medicine, Indianapolis, Indiana 46202, USA. ⁵Division of Allergy, Pulmonary and Critical Care Medicine, Vanderbilt University School of Medicine, Nashville, Tennessee 37232, USA. ⁶Division of Thoracic Surgery, Massachusetts General Hospital, Harvard Medical School, Boston, Massachusetts 02114, USA. ⁷Facultad de Ciencias, Universidad Nacional Autónoma de México, Mexico City, Mexico. ⁸Department of Molecular Biology, Helen L. Dorris Institute for Neurological and Psychiatric Disorders, The Scripps Research Institute, La Jolla, California 92037, USA. ⁹These authors contributed equally to this work. Correspondence should be addressed to A.D.L. (aluster@mgh.harvard.edu).

Received 30 August; accepted 24 October; published online 9 December 2007; doi:10.1038/nm1685

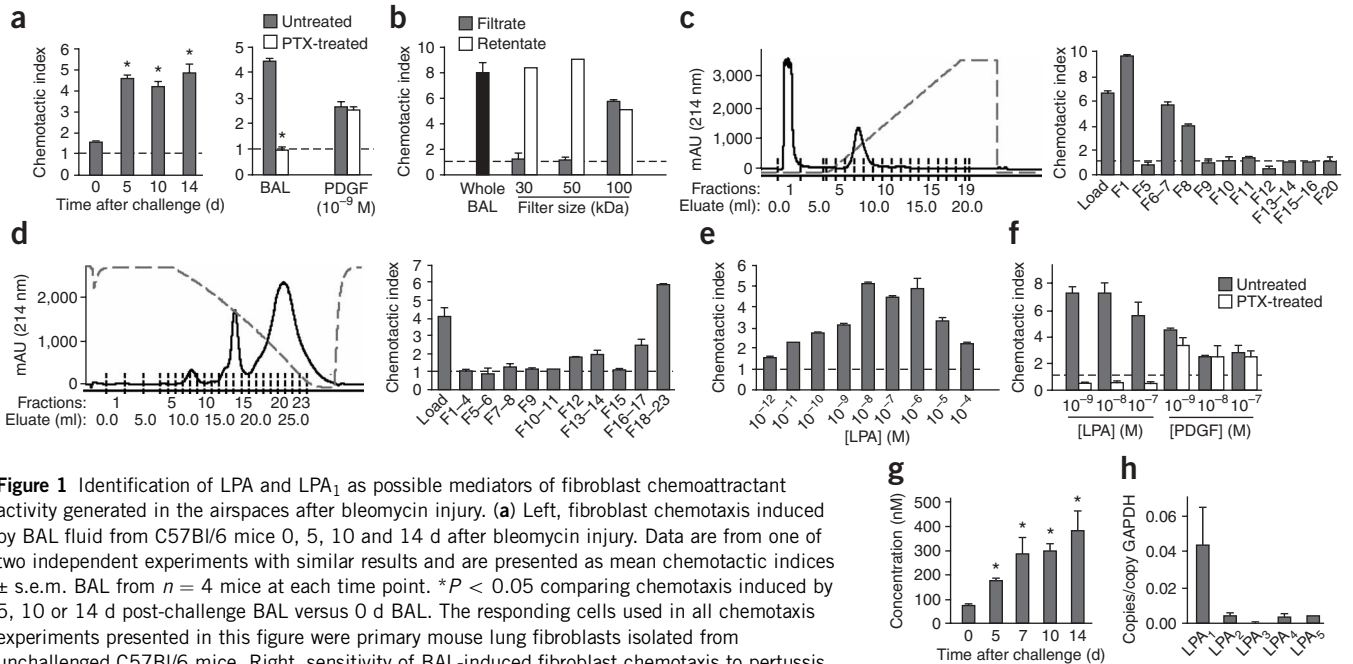


Figure 1 Identification of LPA and LPA₁ as possible mediators of fibroblast chemoattractant activity generated in the airspaces after bleomycin injury. **(a)** Left, fibroblast chemotaxis induced by BAL fluid from C57Bl/6 mice 0, 5, 10 and 14 d after bleomycin injury. Data are from one of two independent experiments with similar results and are presented as mean chemotactic indices \pm s.e.m. from $n = 4$ mice at each time point. $*P < 0.05$ comparing chemotaxis induced by 5, 10 or 14 d post-challenge BAL versus 0 d BAL. The responding cells used in all chemotaxis experiments presented in this figure were primary mouse lung fibroblasts isolated from unchallenged C57Bl/6 mice. Right, sensitivity of BAL-induced fibroblast chemotaxis to pertussis toxin (PTX). 5 d post-bleomycin BAL from $n = 8$ mice. $*P < 0.0001$ comparing chemotaxis induced by 5 d BAL of PTX-treated fibroblasts versus untreated fibroblasts. **(b)** Fibroblast chemotactic indices of filtrates and retentates produced by size-exclusion centrifugation of 5 d post-bleomycin BAL across filters with molecular exclusion sizes of 30, 50 and 100 kDa. Chemotactic index of unfiltered 5 d BAL (black bar) is presented for comparison. **(c)** Heparin affinity chromatography of BAL fibroblast chemoattractants. Left, separation of 5 d post-bleomycin BAL by heparin affinity. Dashed line, eluate conductivity. Right, fibroblast chemotactic indices of heparin affinity fractions. **(d)** Hydrophobic interaction chromatography of BAL fibroblast chemoattractants. Left, separation of 5 d post-bleomycin BAL by hydrophobicity. Dashed line, eluate conductivity. Right, fibroblast chemotactic indices of hydrophobic interaction fractions. **(e)** Fibroblast chemotactic indices induced by LPA. **(f)** Sensitivity of LPA-induced fibroblast chemotaxis to PTX. **(g)** LPA concentrations in BAL after bleomycin injury, $n = 4$ mice per time point. $*P < 0.05$ comparing LPA concentrations of BAL at 5, 7, 10 and 14 d after bleomycin versus 0 d. **(h)** Lung fibroblast LPA receptor expression. Data are presented as copies of receptor mRNA relative to copies of GAPDH mRNA \pm s.e.m. mRNA isolated from $n = 3$ fibroblast cultures, prepared from sets of two C57Bl/6 mice each.

To determine the relevance of our findings to human disease, we investigated the role of the LPA-LPA₁ pathway in fibroblast migration in IPF. We found that LPA levels were elevated in bronchoalveolar lavage (BAL) samples from individuals with IPF and that the fibroblast chemotactic activity present in these samples was dependent on fibroblast LPA₁. On the basis of these findings, we believe that LPA₁ represents a crucial link between lung injury and the development of pulmonary fibrosis.

RESULTS

Fibroblast chemotactic activity generated by lung injury

BAL fluid from mice after bleomycin challenge attracted primary mouse lung fibroblasts, whereas BAL fluid from unchallenged mice did not (**Fig. 1a**). The chemotactic activity of post-challenge BAL was completely inhibited by fibroblast pretreatment with pertussis toxin (PTX, **Fig. 1a**), indicating that the relevant fibroblast receptor(s) signal through the G α_i class of G proteins, a hallmark of the chemoattractant subfamily of GPCRs¹³. In contrast, platelet-derived growth factor (PDGF) signals through receptor tyrosine kinases, and fibroblast chemotaxis induced by this mediator was not inhibited by PTX (**Fig. 1a**). A wide array of chemoattractants signal through PTX-sensitive GPCRs, including chemokines, which we hypothesized were responsible for the post-bleomycin BAL fibroblast chemotactic activity.

Biophysical characterization of BAL fibroblast chemoattractant(s)

We characterized the fibroblast chemoattractant(s) in post-injury BAL by molecular size, heparin binding affinity and hydrophobicity.

After centrifugation of BAL through filters with molecular exclusion sizes of 30 and 50 kDa, the retentates had chemotactic activity equivalent to that of unfiltered BAL, whereas the filtrates had no chemotactic activity (**Fig. 1b**). In contrast, chemotactic activity was present in both the retentate and filtrate produced by a 100-kDa filter. These data indicate that molecule(s) responsible for the chemoattractant activity of BAL fluid have molecular weights between 50 and 100 kDa. When we loaded BAL on a heparin affinity chromatography column, the most abundant proteins either did not bind to the column, or eluted from it at low sodium chloride concentrations, indicating that they had low heparin binding affinities (**Fig. 1c**). Proteins with low heparin affinity that were present in the flow-through (fraction 1) or that eluted in fractions 6, 7 and 8 showed fibroblast chemotactic activity (**Fig. 1c**), whereas proteins with higher heparin affinities did not induce chemotaxis. After we loaded BAL on a hydrophobic interaction chromatography column, the most abundant proteins eluted from the column at low ammonium sulfate concentrations, indicating they had high surface hydrophobicity (**Fig. 1d**). Proteins with high hydrophobicity that eluted in fractions 18–23 showed fibroblast chemotactic activity, whereas proteins with lower hydrophobicity did not induce fibroblast chemotaxis (**Fig. 1d**). Active BAL fractions had low heparin affinity, high hydrophobicity and molecular weights between 50 and 100 kDa, suggesting that the BAL contains fibroblast chemoattractants other than chemokines, which typically are highly charged basic proteins between 8 and 10 kDa in size that have high heparin affinities¹³.

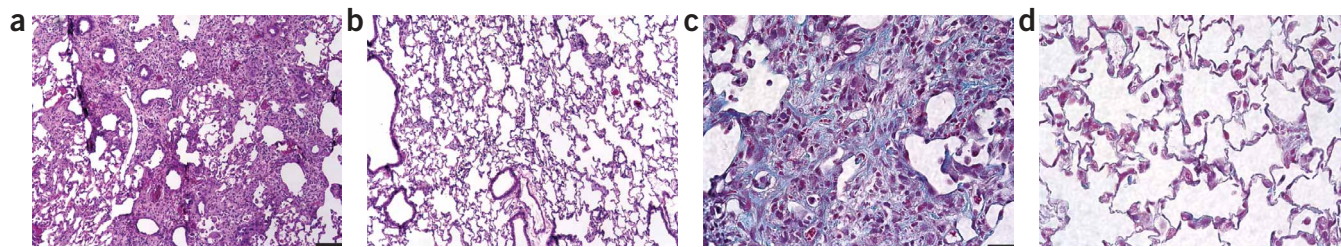
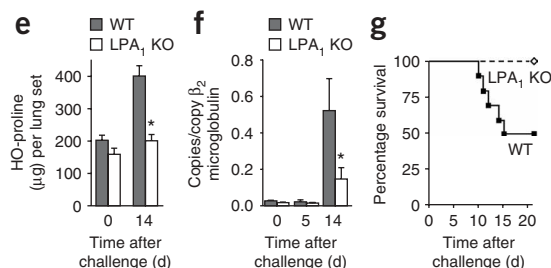


Figure 2 LPA₁-deficient (LPA₁ KO) mice are protected from bleomycin-induced fibrosis and mortality. (a,b) H&E staining of lungs of (a) wild-type and (b) LPA₁ KO mice 14 d after challenge. Bar, 100 μ m. (c,d) Trichrome staining of lungs of (c) wild-type and (d) LPA₁ KO mice 14 d after bleomycin. Bar, 25 μ m. (e) Biochemical analysis of bleomycin-induced fibrosis. Hydroxyproline content was measured in the lungs of wild-type (WT) and LPA₁ KO mice at baseline and 14 d after bleomycin (0 d untreated, $n = 5$ mice/group; 14 d after bleomycin, $n = 8$ mice/group). Data presented are from one of two independent experiments with similar results and are expressed as mean hydroxyproline content per lung set \pm s.e.m. $*P = 0.0073$ for interaction between genotype and bleomycin treatment, as measured by two-way ANOVA for independent samples. (f) Bleomycin-induced expression of procollagen type I α_1 chain mRNA. mRNA

isolated from the lungs of WT and LPA₁ KO mice at baseline ($n = 3$ mice/group) and 5 and 14 d after bleomycin ($n \geq 5$ mice/group). Data are expressed as mean copies of procollagen mRNA relative to copies of β_2 microglobulin mRNA \pm s.e.m. $*P < 0.05$ comparing procollagen expression in WT versus LPA₁ KO lungs at 14 d. (g) Bleomycin-induced mortality. WT and LPA₁ KO mice were followed for survival for 21 d after challenge with 3 units/kg of bleomycin, $n = 10$ mice/group. Significant difference by log-rank test: $P = 0.0115$ LPA₁ KO versus WT survival.



Albumin-bound LPA is a fibroblast chemoattractant

In all BAL separations, active fractions contained an abundant protein the size of mouse albumin (69 kDa), as visualized by SDS-PAGE (Supplementary Fig. 1 online). Albumin transports lipids, which it binds through hydrophobic interactions¹⁴. We hypothesized that a lipid bound to albumin contributed to the BAL fibroblast chemotactic activity. Serum stimulates the formation of actin stress fibers and focal adhesions in fibroblasts. This activity was found to copurify with albumin and, most likely, to be attributable to the albumin-bound lysophospholipid LPA¹⁵. Actin stress fiber and focal adhesion formation are involved in cell migration, and we therefore hypothesized that LPA mediates fibroblast migration induced by BAL after injury. To investigate this hypothesis, we first showed that LPA bound to albumin was chemotactic for primary mouse lung fibroblasts (Fig. 1e). Methanol-extracted fatty acid-free albumin significantly potentiated the chemotactic activity of LPA, by twofold ($P = 0.0058$; Supplementary Fig. 2a online), but did not induce fibroblast chemotaxis by itself (Supplementary Fig. 2b). Chemotaxis induced by LPA was abrogated by fibroblast pretreatment with PTX (Fig. 1f), confirming that the relevant LPA receptor(s) were GPCRs. Chemotactic indices of PTX-treated fibroblasts induced by LPA were actually less than 1, consistent with recently described LPA-mediated inhibition of cell migration through $G\alpha_{12/13}$ -coupled signaling when $G\alpha_i$ -coupled signaling is inhibited by PTX¹⁶.

Electrospray ionization mass spectrometry (ESI-MS) performed on BAL from unchallenged mice (0 d) and mice 5, 7, 10 and 14 d after bleomycin challenge showed that the concentration of LPA in BAL was significantly elevated at all time points after bleomycin injury (Fig. 1g). LPA therefore is present in the BAL at increased levels after bleomycin challenge and is a potent fibroblast chemoattractant. LPA signals through at least five GPCRs designated LPA₁₋₅ (refs. 17–19). The LPA receptor most highly expressed by lung fibroblasts was LPA₁ (Fig. 1h), which has been shown to mediate LPA-induced chemotaxis of mouse embryonic fibroblasts²⁰. Based on these results, we hypothesized that BAL-induced fibroblast chemotaxis is mediated by LPA signaling through LPA₁. To further test this

hypothesis and examine the role of LPA-directed fibroblast recruitment *in vivo*, we obtained mice genetically deficient for LPA₁ (ref. 21) and challenged them with bleomycin.

Bleomycin-induced pulmonary fibrosis is dependent on LPA₁

Lungs 14 d after bleomycin challenge typically show changes consistent with peribronchiolar and parenchymal fibrosis. The extent of these changes present in wild-type mice (Fig. 2a) was substantially decreased in LPA₁-deficient mice (Fig. 2b). The amount of lung collagen visualized by Masson trichrome staining of wild-type mice 14 d after bleomycin challenge (Fig. 2c) was also substantially decreased in LPA₁-deficient mice (Fig. 2d). Assessments of lung collagen at the protein and mRNA levels confirmed the significant protection of LPA₁-deficient mice. As compared to unchallenged mice, the amount of the collagen-specific amino acid hydroxyproline increased by 96% in wild-type mice 14 d after bleomycin challenge but by only 25% in LPA₁-deficient mice (Fig. 2e). mRNA levels of the α_1 gene of procollagen type I increased in the lungs of both genotypes 14 d after challenge, but this increase also was markedly attenuated in LPA₁-deficient mice (Fig. 2f). Finally, at the highest dose of bleomycin challenge used (3 units/kg), the absence of LPA₁ expression substantially protected mice from mortality. At 21 d after challenge, the mortality of wild-type mice was 50%, whereas the mortality of LPA₁-deficient mice was 0% (Fig. 2g).

Bleomycin-induced fibroblast recruitment is dependent on LPA₁

We hypothesized that reduced fibroblast recruitment contributed to the protection of LPA₁-deficient mice from bleomycin-induced fibrosis. To investigate this hypothesis, we first confirmed that LPA₁ mediated LPA-induced chemotaxis of lung fibroblasts by showing that this chemotaxis was abrogated for fibroblasts isolated from LPA₁-deficient mice (Fig. 3a). In contrast, PDGF induced similar chemotaxis of wild-type and LPA₁-deficient fibroblasts (Fig. 3a). We then determined the extent to which fibroblast chemotaxis induced by post-injury BAL was attributable to LPA and LPA₁. The LPA receptor antagonist Ki16425 inhibits LPA-induced responses mediated by

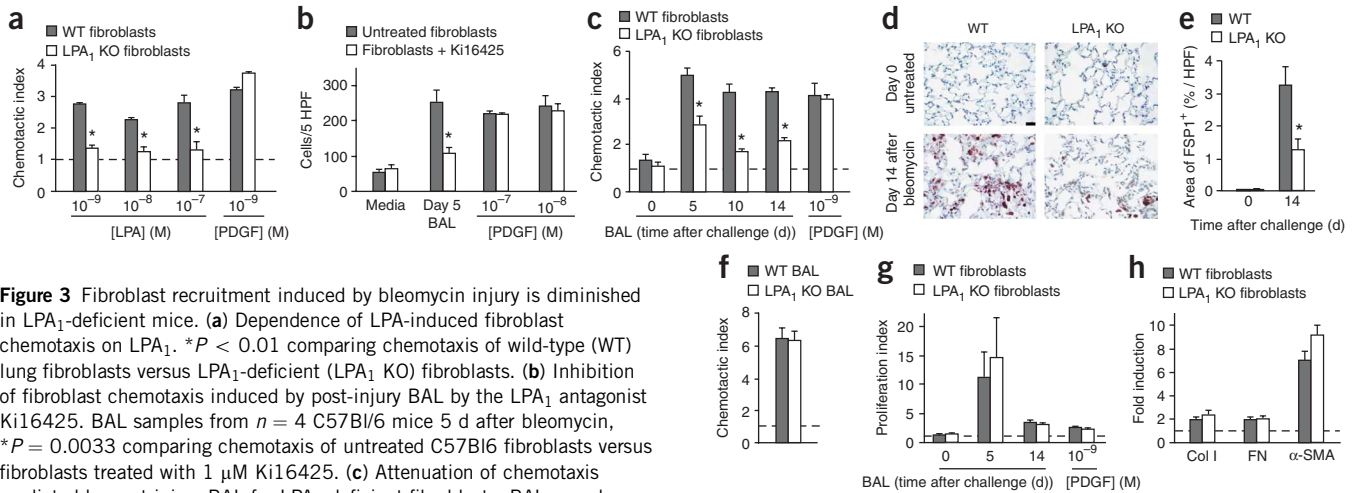


Figure 3 Fibroblast recruitment induced by bleomycin injury is diminished in LPA₁-deficient mice. **(a)** Dependence of LPA-induced fibroblast chemotaxis on LPA₁. **P* < 0.01 comparing chemotaxis of wild-type (WT) lung fibroblasts versus LPA₁ KO fibroblasts. **(b)** Inhibition of fibroblast chemotaxis induced by post-injury BAL by the LPA₁ antagonist Ki16425. BAL samples from *n* = 4 C57Bl/6 mice 5 d after bleomycin, **P* = 0.0033 comparing chemotaxis of untreated C57Bl/6 fibroblasts versus fibroblasts treated with 1 μM Ki16425. **(c)** Attenuation of chemotaxis mediated by post-injury BAL for LPA₁-deficient fibroblasts. BAL samples from *n* = 4 C57Bl/6 mice per time point. **P* < 0.005 comparing chemotaxis of WT versus LPA₁ KO fibroblasts induced by 5, 10 or 14 d after bleomycin BAL. **(d)** Accumulation of FSP1⁺ fibroblasts after bleomycin challenge in WT and LPA₁ KO mice. Lungs of WT and LPA₁ KO mice at baseline (top panels) and 14 d after bleomycin challenge (bottom panels) stained with antibody to FSP1/peroxidase. Bar, 25 μm. **(e)** Lung area comprised of FSP1⁺ cells. Data are expressed as mean FSP1⁺ staining area ± s.e.m.; *n* = 3 mice per group, all groups. **P* = 0.0017, LPA₁ KO 14 d after bleomycin versus WT 14 d after bleomycin. **(f)** Independence of the generation of BAL fibroblast chemotactic activity from LPA₁. BAL samples from *n* = 4 WT and *n* = 4 LPA₁ KO mice 5 d after bleomycin; lung fibroblasts from C57Bl/6 mice. **(g)** Independence of lung fibroblast proliferation induced by post-injury BAL from LPA₁. Data are presented as mean proliferative indices ± s.e.m.; BAL samples from *n* = 3 C57Bl/6 mice per time point after bleomycin; lung fibroblasts from WT and LPA₁ KO mice. **(h)** Independence of lung fibroblast gene expression induced by TGF-β from LPA₁. QPCR analysis of mRNA expression of induced in WT and LPA₁ KO lung fibroblasts by 24 h exposure to TGF-β (10 μg/ml). Data are expressed as fold induction (mean copies of procollagen type I α₁ (Col I), fibronectin (FN) and α-smooth muscle actin (α-SMA) mRNAs relative to copies of β₂ microglobulin mRNA in TGF-β-exposed cells divided by mean copies in nonexposed cells) ± s.e.m. and are from *n* ≥ 3 fibroblasts cultures per genotype per condition.

LPA₁ ≥ LPA₃ >> LPA₂, with a *K_i* value estimated to be 0.25–0.34 μM for LPA₁, without appreciable effects on receptors of closely related lipids, such as sphingosine 1-phosphate (S1P)²². Ki16425 significantly inhibited fibroblast chemotaxis to BAL from mice 5 d after bleomycin challenge (**Fig. 3b**), as did VPC12249 (**Supplementary Fig. 3** online), another specific LPA antagonist that inhibits LPA-induced responses mediated by LPA₁ ≥ LPA₃ >> LPA₂, with a *K_i* value estimated to be 0.14 μM for LPA₁ (ref. 23). Neither antagonist affected PDGF-induced chemotaxis. Chemotaxis induced by BAL from bleomycin-challenged mice was attenuated by more than 50% when the responding cells were LPA₁-deficient fibroblasts. The response of LPA₁-deficient fibroblasts was 45%, 25% and 33% that of wild-type fibroblasts to BAL from mice 5, 10 and 14 d after challenge, respectively (**Fig. 3c**). Given the specificity of LPA₁ for its ligand LPA (reviewed in ref. 17), these data indicate that LPA is the predominant fibroblast chemoattractant recovered from the airspaces throughout the time course of bleomycin-induced fibrosis. The preservation of some chemotactic response of LPA₁-deficient fibroblasts to post-injury BAL, however, indicates that other fibroblast chemoattractants were generated in the injured lung in addition to LPA.

Given our findings that LPA was the predominant fibroblast chemoattractant recovered from the injured lung, and that LPA₁ mediates LPA-induced fibroblast chemotaxis, we hypothesized that the accumulation of fibroblasts would be attenuated in the lungs of LPA₁-deficient mice after bleomycin injury. We first showed that LPA₁ remained highly expressed by lung fibroblasts after bleomycin injury and that LPA₁ deficiency did not cause compensatory changes in the expression of other LPA receptors (**Supplementary Fig. 4** online). We then quantified fibroblast accumulation in wild-type and LPA₁-deficient mice by staining with antibody to fibroblast-specific protein 1 (FSP1)²⁴. Immunohistochemistry previously performed with this antibody specifically stained interstitial cells that

coexpressed procollagen type 1 α₁ (ref. 25). In primary lung cell cultures, fibroblasts but not macrophages or type II alveolar epithelial cells expressed FSP1, suggesting that FSP1 is a useful marker for lung fibroblasts²⁵. Lungs of unchallenged wild-type and LPA₁-deficient mice both contained only very few FSP1⁺ cells (**Fig. 3d**). The number of FSP1⁺ cells increased in both genotypes 14 d after bleomycin, but this increase was attenuated by 62% in LPA₁-deficient mice (**Fig. 3d,e**). If this reduced fibroblast accumulation in LPA₁-deficient mice resulted specifically from impaired fibroblast responsiveness to the chemoattractant activity generated by injury, then the generation of the chemoattractant activity itself should be independent of LPA₁ expression. As predicted, there was no significant difference in the fibroblast chemoattractant activity of BAL fluid from wild-type or LPA₁-deficient mice 5 d after bleomycin challenge (**Fig. 3f**).

We also investigated whether the accumulation of circulating fibroblast precursor cells termed fibrocytes²⁶ was attenuated in the lungs of LPA₁-deficient mice after bleomycin injury. Fibrocytes have been identified as cells that co-stain with antibodies to CD45 and collagen type I (Col I), and they have been shown to be recruited to injured lungs, with peak accumulation occurring approximately 1 week after injury in animal models^{7,27}. We compared the quantities of CD45⁺ Col I⁺ cells present in freshly generated single-cell suspensions of the lungs of LPA₁-deficient and wild-type mice before and 7 d after bleomycin challenge. CD45⁺ Col I⁺ cells represented 0.017% of total cells in both LPA₁-deficient and wild-type mice before bleomycin. The quantities of CD45⁺ Col I⁺ cells in the lungs increased 7 d after challenge similarly in both genotypes, to 0.55% of lung cells in wild-type and to 0.58% in LPA₁-deficient mice (data not shown).

To complement our investigations of fibroblast recruitment, we also investigated whether decreased fibroblast proliferation could contribute to the decreased fibroblast accumulation, and whether decreased collagen production could contribute to the decreased collagen

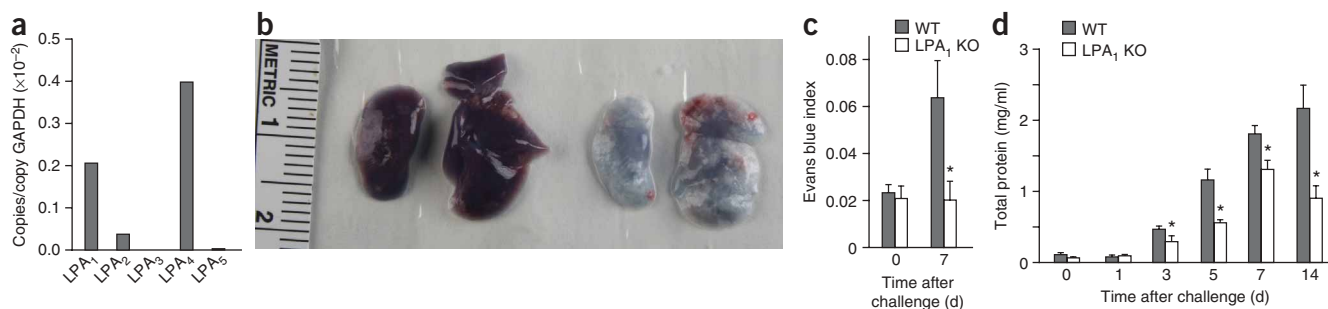


Figure 4 Vascular leak induced by bleomycin injury is diminished in LPA₁-deficient (LPA₁ KO) mice. **(a)** Mouse lung endothelial cell LPA receptor expression. Data are presented as copies of receptor mRNA relative to copies of GAPDH mRNA. **(b)** Assessment of lung vascular permeability by extravasation of Evans blue dye. Gross appearance of lungs from representative wild-type (left) and LPA₁ KO mice (right) 7 d after bleomycin challenge and 3 h after Evans blue injection. **(c)** Evans blue indices of WT and LPA₁ KO mice before and after bleomycin challenge. Lung and plasma samples from $n = 5$ WT mice at each time point, $n = 4$ LPA₁ KO at 0 d and $n = 3$ LPA₁ KO at 7 d. Data presented are from one of three independent experiments with similar results, and are expressed as mean Evans blue index \pm s.e.m. * $P = 0.025$ comparing mean LPA₁ KO index at 7 d versus mean WT index at 7 d. **(d)** Assessment of lung vascular permeability by BAL total protein concentration. BAL samples from $n \geq 4$ WT and LPA₁ KO mice at each time point. Data presented are from one of two independent experiments with similar results and are expressed as mean BAL total protein concentration \pm s.e.m. * $P < 0.05$ comparing LPA₁ KO versus WT protein concentrations at 3, 5, 7 and 14 d after bleomycin.

accumulation, that we observed in bleomycin-challenged LPA₁-deficient mice. There were no significant differences, however, between the proliferative responses of wild-type and LPA₁-deficient fibroblasts to BAL recovered from mice 5 or 14 d after bleomycin challenge (Fig. 3g). Increases in the expression of procollagen type I α_1 and fibronectin induced by transforming growth factor- β (TGF- β) also were similar in wild-type and LPA₁-deficient fibroblasts (Fig. 3h), suggesting that fibroblast synthesis of matrix proteins does not require LPA₁. Induction of fibroblast α -smooth muscle actin expression by TGF- β , a hallmark of myofibroblast differentiation²⁸, was similar in wild-type and LPA₁-deficient fibroblasts as well (Fig. 3h), suggesting that the generation of myofibroblasts also does not require LPA₁.

Reduced accumulation of LPA₁-deficient fibroblasts, rather than impaired capacities to synthesize collagen or differentiate into myofibroblasts, therefore contributed to reduced collagen accumulation after lung injury in LPA₁-deficient mice. Reduced fibroblast accumulation in LPA₁-deficient mice in turn resulted from reduced migration of LPA₁-deficient fibroblasts to the chemoattractant activity induced by lung injury, rather than from impaired generation of this activity or from reduced fibroblast proliferation.

Bleomycin-induced vascular leak is dependent on LPA₁

We hypothesized that reduced vascular leak also contributed to the protection from bleomycin-induced fibrosis that we observed in LPA₁-deficient mice. We determined that of the five different LPA receptors, primary mouse lung endothelial cells predominantly expressed LPA₁ and LPA₄ (Fig. 4a). We then compared injury-induced vascular leak in LPA₁-deficient versus wild-type mice by comparing Evans blue dye extravasation and BAL total protein concentration in these mice after bleomycin challenge. At 7 d after injury, increased vascular permeability in wild-type mice enabled Evans blue dye to extravasate from the vasculature into the lung parenchyma, turning these lungs deep purple (Fig. 4b). Much less dye extravasated into the lung parenchyma of LPA₁-deficient mice, turning their lungs only pale blue (Fig. 4b), indicative of reduced vascular leak. The extravasation of Evans blue dye was significantly increased in wild-type mice 7 d after bleomycin challenge compared to unchallenged mice, whereas this increase was almost completely abrogated in LPA₁-deficient mice (Fig. 4c). The increased BAL total protein concentration that

occurs after bleomycin injury in wild-type mice was also significantly reduced in LPA₁-deficient mice at 3, 5, 7 and 14 d after bleomycin challenge (Fig. 4d).

Leukocyte recruitment is not dependent on LPA₁

LPA is a chemoattractant for multiple leukocyte subsets^{29,30}. If LPA contributed to leukocyte recruitment after bleomycin injury, then reduced leukocyte accumulation in LPA₁-deficient mice could also contribute to their protection from bleomycin-induced fibrosis. We determined the LPA receptor expression of leukocyte subsets that are recruited into the lung after bleomycin injury, including both myeloid and lymphoid lineages. Alveolar macrophages, neutrophils and CD4⁺ and CD8⁺ T cells all expressed minimal LPA₁ and substantially greater amounts of other LPA receptors (Fig. 5a). Consistent with this receptor expression profile, there were no significant differences in the numbers of total leukocytes (Fig. 5b), macrophages (Fig. 5c) or neutrophils (Fig. 5d) that were present in the BAL of LPA₁-deficient and wild-type mice at 1, 3, 5 and 7 d after challenge. The numbers of CD3⁺ T cells (Fig. 5e), CD4⁺ T cells (Fig. 5f) and CD8⁺ T cells (Fig. 5g) were also similar in LPA₁-deficient and wild-type mice at 3, 5 and 7 d after bleomycin challenge. Leukocyte recruitment was ultimately attenuated, however, in LPA₁-deficient mice at 14 d after bleomycin challenge, consistent with faster resolution of repair processes in the setting of diminished fibrosis. We also compared the functional phenotype and activation status of lymphocytes recruited into the lungs of LPA₁-deficient and wild-type mice after bleomycin challenge. At 5 d after bleomycin challenge, almost all CD4⁺ and CD8⁺ T cells recovered in BAL from both LPA₁-deficient and wild-type mice had a memory phenotype, as indicated by high CD44 expression (Fig. 5h)³¹. The percentages BAL CD4⁺ and CD8⁺ T cells that had recently been activated, as indicated by CD69 expression^{32,33}, were also similar in LPA₁-deficient and wild-type mice (Fig. 5h). These data indicate that leukocyte recruitment and activation after bleomycin challenge initially occur independently of LPA₁ and that the inflammatory and fibrotic responses to lung injury are uncoupled in the absence of LPA₁ expression.

LPA and LPA₁ in human fibrotic lung disease

To determine the relevance of our studies in the bleomycin mouse model to human disease, we investigated the role of the LPA-LPA₁

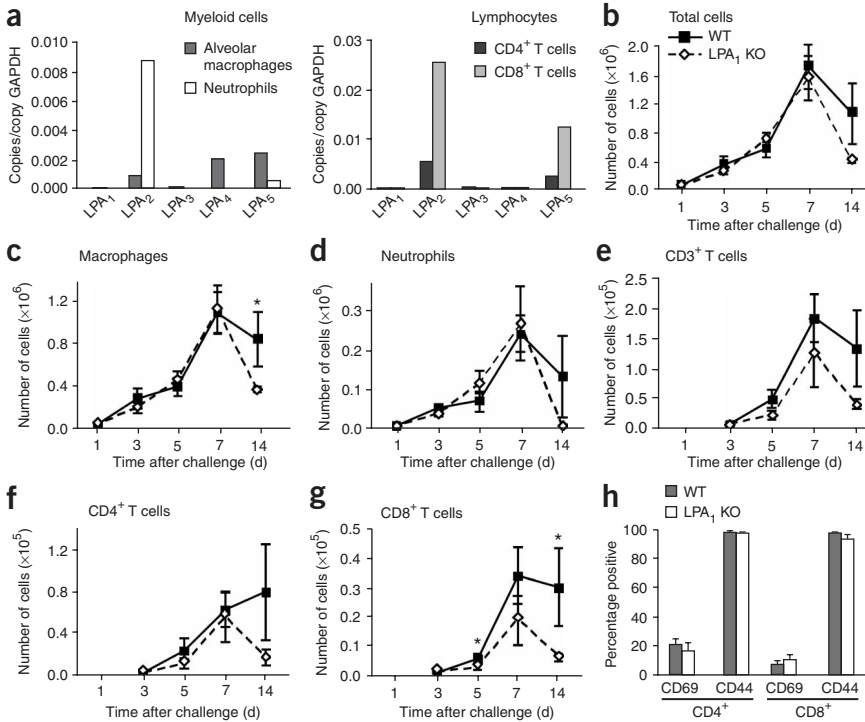


Figure 5 Leukocyte recruitment and activation induced by bleomycin injury is preserved in LPA₁-deficient (LPA₁ KO) mice. **(a)** LPA receptor expression of myeloid cells (left) and lymphocytes (right). Data are presented as copies of receptor mRNA relative to copies of GAPDH mRNA. **(b)** BAL total cell numbers were determined from $n = 4$ mice per genotype per time point. Data presented are from one of two independent experiments, and are expressed as mean cell numbers \pm s.e.m. **(c,d)** BAL myeloid cell numbers. Numbers of BAL **(c)** macrophages and **(d)** neutrophils were determined from $n = 4$ mice per genotype per time point. $*P < 0.05$ comparing wild-type (WT) versus LPA₁ KO BAL macrophages 14 d after bleomycin. **(e-g)** BAL T cell numbers. Numbers of **(e)** T cells (CD3⁺), **(f)** CD4⁺ T cells (CD3⁺CD4⁺) and **(g)** CD8⁺ T cells (CD3⁺CD8⁺) were determined from $n = 4$ mice per genotype per time point. $*P < 0.05$ comparing WT versus LPA₁ KO BAL CD8⁺ T cells at 5 and 14 d post-bleomycin. **(h)** BAL T cell functional phenotype and activation status. Percentages of CD4⁺ and CD8⁺ T cells in BAL from WT and LPA₁ KO mice 5 d after bleomycin challenge that were CD69⁺ and CD44⁺ were determined. Data are presented as mean percentages positive \pm s.e.m.

pathway in fibroblast migration in IPF, a prototypic human fibrotic lung disease. Fibroblasts that have migrated into the airspaces can be recovered in BAL samples of persons with pulmonary fibrosis, but not healthy persons³⁴. We found that LPA₁ was the LPA receptor that was most highly expressed by fibroblasts grown from human IPF BAL (Fig. 6a). The expression of collagen type I α_1 by these cells was much greater than their expression of CD14, consistent with these cells being fibroblasts (or fibrocytes) rather than macrophages, the most likely contaminating cell type (Fig. 6b).

We then determined LPA levels in the BAL fluid of persons with IPF, and investigated whether fibroblast migration induced by IPF BAL is dependent on LPA₁. As determined by ESI-MS, total LPA concentrations in BAL samples from individuals with IPF were significantly higher than concentrations in BAL from normal controls (Fig. 6c). In chemotaxis experiments using human fetal lung fibroblasts (HFL1 cells) as the responding cells, we found that BAL fluid from people with IPF induced significantly greater fibroblast

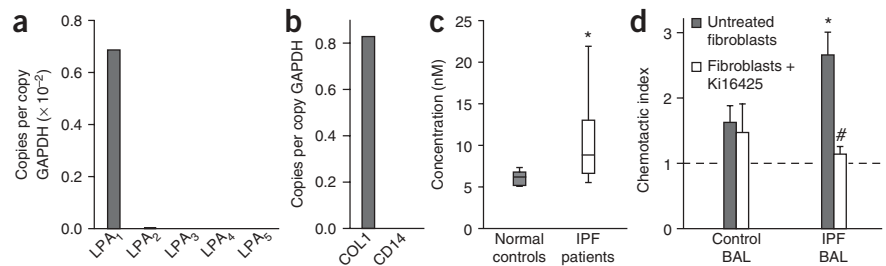
chemotaxis than BAL from controls (Fig. 6d). Further, the LPA₁ antagonist Ki16425 markedly inhibited fibroblast chemotaxis induced by IPF BAL samples (Fig. 6d), indicating that fibroblast migration induced by BAL from people with IPF is mediated by the LPA-LPA₁ pathway.

DISCUSSION

We found that the fibroblast chemotactic activity of BAL fluid from bleomycin-injured mice copurified with albumin, leading us to hypothesize that this activity was attributable to albumin-bound LPA. After establishing that LPA was chemotactic for primary lung fibroblasts, that LPA was generated in the airspaces after bleomycin injury and that LPA₁ was the predominant LPA receptor expressed by lung fibroblasts, we challenged LPA₁-deficient mice with bleomycin and found that they were markedly protected from pulmonary fibrosis. In addition to mitigating the excessive accumulation of fibroblasts in the injured lung, the absence of LPA₁ markedly

Figure 6 LPA and LPA₁ contribute to the fibroblast chemoattractant activity of BAL from persons with IPF. **(a,b)** LPA receptor expression **(a)** and procollagen type I α_1 (Col I) and CD14 expression **(b)** of fibroblasts grown from BAL of an individual with IPF. Data are presented as copies of mRNA of the gene of interest relative to copies of GAPDH mRNA. **(c)** LPA concentrations in BAL from persons with IPF. Concentrations of LPA were determined in BAL from individuals with IPF ($n = 9$) and normal controls ($n = 7$) collected either at the Instituto Nacional de

Enfermedades Respiratorias (INER), México or the Massachusetts General Hospital (MGH). Data are presented as box and whisker plots, in which the horizontal line within each box represent the median, the limits of each box represent the interquartile range and the whiskers represent the maximum and minimum values. $*P = 0.029$ comparing LPA concentrations of affected versus unaffected individuals. **(d)** Induction of fibroblast chemotaxis by IPF BAL and its inhibition by the LPA₁ antagonist Ki16425. BAL samples were from persons with IPF ($n = 7$) and controls ($n = 3$) collected at the INER; responding cells were human fetal lung fibroblasts (HFL1 cells). $*P < 0.05$ comparing chemotaxis induced by IPF versus control BAL samples; $\#P < 0.0005$ comparing chemotaxis induced by IPF BAL for untreated HFL1 cells versus HFL1 cells treated with 1 μ M Ki16425.



attenuated the persistent vascular leak produced by injury, indicating that the LPA-LPA₁ pathway mediates both of these aberrant wound-healing responses that have been implicated in pulmonary fibrosis. Showing that this novel pathway identified in the bleomycin model is relevant to human fibrotic lung disease, BAL LPA levels were greater in persons with IPF than in normal controls, and inhibition of LPA signaling markedly reduced fibroblast responses to IPF BAL chemoattractant activity.

Fibroblast migration into the fibrin provisional wound matrix is a central step in wound-healing responses to injury in multiple tissues². In the lung, fibroblasts migrate into the fibrin-rich exudates that develop in the airspaces after lung injury^{3,35}. Fibroblast chemoattractant activity has previously been shown to be generated in the airspaces of persons with IPF, and the extent of this activity has been found to inversely correlate with affected individuals' total lung capacity and vital capacity⁴. In a recent evaluation of the clinical and molecular features of 'rapid' and 'slow' progressors with IPF, evidence of increased fibroblast migration was associated with an accelerated clinical course and higher mortality⁵. Our results show that LPA is the predominant mediator of fibroblast migration generated in the injured lung that is recovered in BAL. Determining whether the higher BAL fibroblast chemoattractant activity found in 'rapid' progressors with IPF is attributable to higher LPA levels in their BALs will be of great interest, and will be the focus of future studies.

Our results also indicate that other fibroblast chemoattractants in addition to LPA are generated after lung injury, and that in contrast to fibroblasts, bleomycin-induced accumulation of fibrocytes was not affected by the absence of LPA₁ expression. These data suggest that different chemoattractants may cooperate in fibroblast recruitment after lung injury, with different chemoattractants mediating different steps in this process. Whereas chemokines such as CXCL12 (ref. 7) and CCL12 (ref. 8) have been found to direct the trafficking of fibrocytes from the bone marrow and/or circulation to the lungs after injury, LPA may act cooperatively with these chemokines by directing the invasion of these cells, or the fibroblasts that derive from them, into the airspaces. LPA has been shown to induce the invasion of cancer cells across tissue barriers, promoting metastasis³⁶, and may analogously direct the invasion of fibroblasts across alveolar basement membranes into injured airspaces³.

Increased vascular permeability is another hallmark of tissue injury². Tissue injury can directly disrupt blood vessels, but it also results in the production of bioactive mediators that cause increased vascular permeability to continue throughout early phases of tissue repair¹¹. Our results indicate that LPA signaling through LPA₁ expressed by endothelial cells mediates the increased vascular permeability that persists after lung injury. In this regard, LPA acts in opposition to another lysophospholipid, S1P, which reduces vascular leak after lung injury³⁷. S1P signals through GPCRs designated S1P₁₋₅, which share homology with LPA₁₋₃ (ref. 17).

One consequence of the persistent vascular leak induced by lung injury that may contribute to the development of fibrosis is extravascular coagulation^{12,38}. Fibrin deposition in injured airspaces may contribute to fibroblast accumulation both by providing a provisional matrix for fibroblast migration and by promoting epithelial-to-mesenchymal transition³⁹. Several proteases of the extrinsic coagulation cascade, such as thrombin, also signal through protease-activated receptors, and they may promote fibrosis independently of fibrin generation through the induction of mediators such as PDGF³⁸. Excessive extravascular coagulation may therefore contribute to lung fibrosis after injury through multiple mechanisms.

In contrast to reduced fibroblast recruitment and vascular leak, we found that other processes involved in wound healing were preserved in LPA₁-deficient mice, including fibroblast proliferation and expression of matrix components, myofibroblast differentiation and leukocyte recruitment. The potential contributions of LPA signaling to processes involved in wound healing that we have not yet investigated, such as apoptosis of injured cells and activation of TGF- β , will be the focus of future studies. The preservation of leukocyte recruitment and activation in the first week after bleomycin challenge in LPA₁-deficient mice indicates that these processes initially occur independently of LPA₁. The occurrence of reduced fibrosis in LPA₁-deficient mice despite inflammatory leukocyte responses similar to those of wild-type mice indicates that inflammatory and fibrotic responses to lung injury were uncoupled in the absence of LPA₁ expression in this model. The dissociation of inflammatory and fibrotic responses to bleomycin injury has been noted previously in other genetically altered mice, such as mice deficient for the integrin β 6 (ref. 40). This dissociation of fibrosis from inflammation in the bleomycin model has provided supporting evidence that in fibrotic diseases resulting from lung injury, inflammation may not be absolutely required for the development of pulmonary fibrosis¹.

Several processes induced by lung injury may contribute to increased levels of LPA in the airspaces, including platelet activation⁴¹ and hydrolysis of surfactant phospholipids⁴². In addition to the regulation of LPA concentration, however, LPA activity is also regulated by its binding to proteins that can either sequester it or increase its delivery to its receptors⁴³. Some of the biological activities of LPA are potentiated by its binding to albumin. An example of a protein that can inhibit LPA activity is plasma gelsolin⁴³. Plasma gelsolin levels decline after tissue injury, and increased LPA activity due to plasma gelsolin depletion has been hypothesized to exacerbate organ dysfunction in this setting⁴⁴. These studies suggest that the increased fibroblast chemotactic activity of BAL samples from bleomycin-injured mice and persons with IPF may result from increased LPA activity due to the combination of increased LPA levels, increased levels of albumin and decreased levels of proteins that inhibit LPA activity.

In this study, we have shown that LPA signaling through its receptor LPA₁ mediates both fibroblast recruitment and vascular leak produced by lung injury in the bleomycin model of pulmonary fibrosis. The concurrent mitigation of these two tissue responses to injury may explain the marked protection of LPA₁-deficient mice from fibrosis in this model. The relevance of this novel pathway to human fibrotic lung disease is shown by the presence of increased LPA levels in BAL fluid of persons with IPF and by the dependence of fibroblast migration induced by IPF BAL on LPA-LPA₁ signaling. These results suggest that LPA₁ may be a promising new therapeutic target for an entire class of diseases in which aberrant responses to injury contribute to the development of fibrosis, such as IPF.

METHODS

Animals and bleomycin administration. We purchased wild-type C57Bl/6 mice from Charles River Breeding Laboratories. Experiments comparing LPA₁-deficient and wild-type mice used sex- and age- or weight-matched groups produced by mating mice heterozygous for the LPA₁ mutant allele that were hybrids of the C57Bl/6 and 129Sv/J genetic backgrounds²¹. These mice consequently on average had similar assortments of genes from the C57Bl/6 and 129Sv/J backgrounds. C57Bl/6 mice received total doses of 0.05 or 0.075 units of bleomycin (Gensia Sciro Pharmaceuticals) by intratracheal injection. We challenged LPA₁-deficient and littermate wild-type mice with doses of bleomycin that were similar to those given C57Bl/6 mice, but that were adjusted for weight: 2 or 3 units of bleomycin per kg body weight. We performed all experiments in accordance with National Institute of Health

guidelines and protocols approved by the Massachusetts General Hospital Subcommittee on Research Animal Care, and maintained all mice in a specific pathogen-free (SPF) environment certified by the American Association for Accreditation of Laboratory Animal Care (AAALAC).

Mouse BAL recovery and fractionation. To obtain BAL samples for analysis of chemoattractant activity and for determination of LPA and total protein concentrations, we lavaged lungs with two 0.5-ml aliquots of PBS. We centrifuged these BAL samples at 3,000g for 20 min at 4 °C and transferred the supernatants to siliconized low-binding Eppendorf tubes (PGC Scientifics) for subsequent analysis. To obtain BAL samples for analysis of leukocyte recruitment, we lavaged lungs with six 0.5-ml aliquots of PBS BAL fluid. We centrifuged these samples at 540g at 4 °C and resuspended the pelleted cells for cytosin and cytofluorimetric analysis. We performed size-exclusion centrifugation of BAL with Microcon Centrifugal Filter Units (Millipore) with molecular-weight exclusion sizes of 30, 50 and 100 kDa. We performed heparin affinity chromatography by loading BAL onto a 5-ml HiTrap Heparin HP column (Amersham Biosciences) equilibrated in 50 mM sodium acetate, pH 4.5, and eluted it with a linear gradient of 0–2 M NaCl in 50 mM sodium acetate, pH 4.5, using an ÄKTA FPLC system (Amersham Biosciences). We performed hydrophobic interaction chromatography by dialyzing BAL against 50 mM sodium phosphate buffer, 1.7 M ammonium sulfate, pH 7.0, loading onto a 1-ml RESOURCE PHE column (Amersham Biosciences) equilibrated in the same buffer, and eluting with a linear gradient of 1.7–0.0 M ammonium sulfate. Before use in chemotaxis assays, we washed heparin binding affinity and surface hydrophobicity fractions with PBS and returned them to their original volumes using Centricon Centrifugal Filter Units with molecular-weight exclusion size of 3 kDa. We visualized proteins in size exclusion centrifugation, heparin binding affinity and surface hydrophobicity fractions by SDS-PAGE (4–20% Tris-HCl gels, Bio-Rad) and Coomassie staining.

Isolation of primary mouse lung fibroblasts, endothelial cells and leukocyte subsets. We isolated primary lung fibroblasts as previously described⁶. We isolated primary lung endothelial cells by sequential selection with PECAM-1-specific and ICAM-2-specific monoclonal antibody-coated magnetic beads according to a published protocol⁴⁵. Alveolar macrophages represented >95% of cells in the BAL of unchallenged C57Bl/6 mice, and we recovered them as described above. We isolated >90% pure populations of mature neutrophils from the bone marrow of unchallenged C57Bl/6 mice by centrifugation over discontinuous Percoll gradients as previously described⁴⁶. We isolated CD4⁺ and CD8⁺ T cells from spleen and pooled cervical, axillary and inguinal lymph nodes using mouse CD4 and CD8 Dynabeads, respectively (Dyna).

Fibroblast chemotaxis assays. We performed fibroblast chemotaxis assays with primary mouse lung fibroblasts or human fetal lung fibroblasts (HFL1 cells, American Type Culture Collection) as previously described⁶, using BAL or BAL fractions, 18:1 LPA (Avanti Polar Lipids) or PDGF-BB (R&D Systems) as chemoattractants. We determined chemotactic indices as the ratio of cells counted in duplicate wells moving in response to a chemoattractant relative to cells moving in response to media control. To chemically inhibit LPA₁ in these experiments with Ki16425 (Sigma), we pretreated the responding fibroblasts with 1 μM Ki16425 for 30 min before the assay and added the same concentration of Ki16425 to the BAL samples used as chemoattractants. To chemically inhibit LPA₁ in these experiments with VPC12249 (gift of K.R. Lynch, University of Virginia), we added 100 μM VPC12249 to the chemoattractants.

BAL LPA analysis. An investigator blinded to the identity of the samples determined BAL total LPA concentrations by electrospray ionization mass spectrometry (ESI-MS) as previously described⁴⁷.

RNA analysis. We isolated total cellular RNA from primary cells using RNeasy Mini kits (Qiagen). We isolated total cellular RNA from lung tissue disrupted by Polytron in TRIzol reagent (Invitrogen). We performed quantitative real-time PCR (QPCR) analysis using an Mx4000 Multiplex Quantitative PCR System (Stratagene) as previously described⁴⁸.

Histopathological and immunohistochemical examination. We fixed lungs excised for histopathology with 10% buffered formalin. We stained multiple paraffin-embedded 5-μm sections of the entire mouse lung with H&E or Masson trichrome. We performed FSP1 immunostaining as previously described²⁵ and quantified the staining using IPLab image analysis software (Scanalytics). We determined the area of FSP1 staining as a percentage of a lung high-power field (HPF) for ten randomly selected nonoverlapping HPFs for each lung section.

Hydroxyproline assay. We measured lung hydroxyproline as previously described⁶.

Fibroblast proliferation. We seeded primary mouse lung fibroblasts into 24-well plates (4 × 10⁴ fibroblasts/well), and after 8 h in culture, deprived them of serum overnight. We then added BAL (diluted 1:4 in serum-free DMEM) or PDGF-BB to the cells for a total of 32 h, and determined proliferation by incorporation of [methyl-³H]thymidine (DuPont-NEN) during the final 8 h. We determined proliferative indices as CPM incorporated into cells proliferating in response to BAL or PDGF counted in triplicate wells relative to CPM incorporated into cells proliferating in media control.

Evans blue dye extravasation assay. We assessed extravasation of Evans blue dye using a technique modified from a previously published technique⁴⁹. Briefly, we injected Evans blue dye (20 mg/kg; Sigma) intravenously into mice 3 h before they were killed. At the time of killing, we recovered blood into a heparinized syringe by cardiac puncture. We then perfused the right ventricle with PBS to remove intravascular dye from the lungs, which we then removed and homogenized. We extracted Evans blue by the addition of two volumes of formamide followed by incubation overnight at 60 °C, followed by centrifugation at 5,000g for 30 min. The absorption of Evans blue in lung supernatants and plasma was measured at 620 nm and corrected for the presence of heme pigments as follows: $A_{620}(\text{corrected}) = A_{620} - (1.426 \times A_{740} + 0.030)$ ⁴⁹. We calculated an Evans blue index as the ratio of the amount of dye in the lungs to the plasma dye concentration.

BAL total protein. We determined total protein concentrations in BAL samples using a commercially available bicinchoninic acid BCA Protein Assay Kit (Pierce).

BAL leukocyte counts and cytofluorimetry. We enumerated BAL leukocytes by trypan blue exclusion using a hemacytometer. We determined percentages of macrophages and neutrophils on preparations of cells centrifuged with a Cytospin 3 (Shandon) and stained them with Hema 3 stain. We generated numbers of macrophages and neutrophils by multiplying their percentages by total BAL cell counts. We incubated cells recovered from BAL at 4 °C for 20 min with 2.4G2 antibody to FcγIII/II receptor (BD Pharmingen), and we stained with monoclonal antibodies to mouse CD3, CD4, CD8, CD44 and/or CD69 that were directly conjugated to fluorescein isothiocyanate, phycoerythrin or allophycocyanin (all from BD Pharmingen) at 4 °C for 30 min. We determined percentages of CD3⁺, CD4⁺, CD8⁺, CD44⁺ and CD69⁺ cells by cytofluorimetry performed using a FACSCalibur Cytometer (Becton-Dickinson) and analyzed them using CellQuest software. We generated numbers of CD3⁺, CD4⁺ and CD8⁺ cells by multiplying their percentages by total BAL cell counts.

Human BAL and BAL fibroblasts. We recovered BAL samples from persons with IPF and normal controls after instillation of sterile 0.9% saline by flexible fiber-optic bronchoscopy. We performed these bronchoscopies both at the Instituto Nacional de Enfermedades Respiratorias (INER), México and the Massachusetts General Hospital (MGH), as previously described^{5,50}. These studies were approved by the INER Ethics Committee and the MGH Institutional Review Board, and informed consent was obtained from all participants. We immediately transferred BAL supernatants that were collected at MGH to siliconized low-binding Eppendorf tubes, and we kept supernatants at both institutions at –70 °C until use. We plated the pelleted cells that we recovered from BAL performed at the MGH in DMEM with 20% (vol/vol) FBS and

incubated them at 37 °C in 5% CO₂. We characterized cells growing at passage 3 or higher as primary human BAL fibroblasts.

Statistical analysis. We tested differences in fibroblast chemotactic and proliferative indices, BAL LPA and total protein concentrations, lung FSP1⁺ staining areas, lung or fibroblast gene expression, Evans blue indices and BAL leukocyte counts between wild-type and LPA₁-deficient mice or fibroblasts for statistical significance by Student's *t*-test using Microsoft Excel software. We tested effects of genotype and bleomycin challenge on lung hydroxyproline for statistically significant interaction by two-way analysis of variance for independent samples using VassarStats (<http://faculty.vassar.edu/lowry/VassarStats.html>). Differences in survival between wild-type and LPA₁-deficient mice were tested for statistical significance by log-rank test. *P* < 0.05 was considered significant in all comparisons.

Note: Supplementary information is available on the Nature Medicine website.

ACKNOWLEDGMENTS

The authors gratefully acknowledge that these studies were supported by a Pulmonary Fibrosis Foundation Grant, an American Lung Association Dalsemer Grant, and a Nirenberg Center for Advanced Lung Disease Grant (to A.M.T.), by Universidad Nacional Autónoma de México Grant SDLPTID.05.6 (to M.S. and A.P.) and by US National Institutes of Health grants R01-CA89228 and R01-CA095042 (to Y.X.), R01-MH51699, K02-MH01723 and R01-NS048478 (to J.C.) and R01-CA69212 (to A.D.L.). The authors thank C.P. Leary for her assistance, S.D. Bercury, E.C. Poorvu and S.F. Brooks for their technical assistance, and K.R. Lynch for the gift of VPC12249.

AUTHOR CONTRIBUTIONS

A.M.T. conceived the idea for the study, designed, directed and interpreted all of the experiments, and prepared the manuscript. P.L. performed and analyzed the experiments comparing fibrosis and mortality in LPA₁-deficient and wild-type mice. P.L. and B.S.S. performed and analyzed the experiments comparing fibroblast accumulation and vascular leak in LPA₁-deficient and wild-type mice. P.L., B.S.S., B.A.K.-S. and W.K.H. performed and analyzed the experiments comparing leukocyte recruitment in LPA₁-deficient and wild-type mice. G.S.C. performed and analyzed the chromatography and SDS-PAGE experiments. M.S., J.W., A.P., B.S.S. and A.M.T. collected and provided the human BAL samples. Z.Z. and Y.X. performed and analyzed the mass spectrometry experiments. V.P. and T.S.B. performed and analyzed the FSP1 staining. N.D.K. isolated and provided the primary mouse lung endothelial cells and mouse neutrophils. W.K.H. performed the chemotaxis and QPCR experiments. J.C. provided the LPA₁-deficient mice. P.L., B.S.S., M.S. A.P., T.S.B., Y.X., and J.C. provided critical review and comments on the manuscript. A.D.L. supervised all aspects of the study, including experimental design, data interpretation, and manuscript preparation.

Published online at <http://www.nature.com/naturemedicine>

Reprints and permissions information is available online at <http://npg.nature.com/reprintsandpermissions>

- Selman, M., King, T.E. & Pardo, A. Idiopathic pulmonary fibrosis: prevailing and evolving hypotheses about its pathogenesis and implications for therapy. *Ann. Intern. Med.* **134**, 136–151 (2001).
- Martin, P. Wound healing—aiming for perfect skin regeneration. *Science* **276**, 75–81 (1997).
- Kuhn, C. *et al.* An immunohistochemical study of architectural remodeling and connective tissue synthesis in pulmonary fibrosis. *Am. Rev. Respir. Dis.* **140**, 1693–1703 (1989).
- Behr, J. *et al.* Fibroblast chemotactic response elicited by native bronchoalveolar lavage fluid from patients with fibrosing alveolitis. *Thorax* **48**, 736–742 (1993).
- Selman, M. *et al.* Accelerated variant of idiopathic pulmonary fibrosis: clinical behavior and gene expression pattern. *PLoS ONE* **2**, e482 (2007).
- Tager, A.M. *et al.* Inhibition of pulmonary fibrosis by the chemokine IP-10/CXCL10. *Am. J. Respir. Cell Mol. Biol.* **31**, 395–404 (2004).
- Phillips, R.J. *et al.* Circulating fibrocytes traffic to the lungs in response to CXCL12 and mediate fibrosis. *J. Clin. Invest.* **114**, 438–446 (2004).
- Moore, B.B. *et al.* The Role of CCL12 in the Recruitment of Fibrocytes and Lung Fibrosis. *Am. J. Respir. Cell Mol. Biol.* **35**, 175–181 (2006).
- van Nieuw Amerongen, G.P., Vermeer, M.A. & van Hinsbergh, V.W. Role of RhoA and Rho kinase in lysophosphatidic acid-induced endothelial barrier dysfunction. *Arterioscler. Thromb. Vasc. Biol.* **20**, E127–E133 (2000).
- Neidlinger, N.A., Larkin, S.K., Bhagat, A., Victorino, G.P. & Kuypers, F.A. Hydrolysis of phosphatidylserine-exposing red blood cells by secretory phospholipase A2 generates lysophosphatidic acid and results in vascular dysfunction. *J. Biol. Chem.* **281**, 775–781 (2006).
- Dvorak, H.F. Tumors: wounds that do not heal. Similarities between tumor stroma generation and wound healing. *N. Engl. J. Med.* **315**, 1650–1659 (1986).
- Idell, S. Coagulation, fibrinolysis, and fibrin deposition in acute lung injury. *Crit. Care Med.* **31**, S213–S220 (2003).
- Luster, A.D. Chemokines—chemotactic cytokines that mediate inflammation. *N. Engl. J. Med.* **338**, 436–445 (1998).
- Curry, S., Brick, P. & Franks, N.P. Fatty acid binding to human serum albumin: new insights from crystallographic studies. *Biochim. Biophys. Acta* **1441**, 131–140 (1999).
- Ridley, A.J. & Hall, A. The small GTP-binding protein rho regulates the assembly of focal adhesions and actin stress fibers in response to growth factors. *Cell* **70**, 389–399 (1992).
- Sugimoto, N., Takawa, N., Yoshioka, K. & Takawa, Y. Rho-dependent, Rho kinase-independent inhibitory regulation of Rac and cell migration by LPA1 receptor in Gi-inactivated CHO cells. *Exp. Cell Res.* **312**, 1899–1908 (2006).
- Ishii, I., Fukushima, N., Ye, X. & Chun, J. Lysophospholipid receptors: signaling and biology. *Annu. Rev. Biochem.* **73**, 321–354 (2004).
- Noguchi, K., Ishii, S. & Shimizu, T. Identification of p2y9/GPR23 as a novel G protein-coupled receptor for lysophosphatidic acid, structurally distant from the Edg family. *J. Biol. Chem.* **278**, 25600–25606 (2003).
- Lee, C.W., Rivera, R., Gardell, S., Dubin, A.E. & Chun, J. GPR92 as a new G(12/13)- and G(q)-coupled lysophosphatidic acid receptor that increases cAMP, LPA5. *J. Biol. Chem.* **281**, 23589–23597 (2006).
- Hama, K. *et al.* Lysophosphatidic acid and autotaxin stimulate cell motility of neoplastic and non-neoplastic cells through LPA1. *J. Biol. Chem.* **279**, 17634–17639 (2004).
- Contos, J.J., Fukushima, N., Weiner, J.A., Kaushal, D. & Chun, J. Requirement for the LPA1 lysophosphatidic acid receptor gene in normal suckling behavior. *Proc. Natl. Acad. Sci. USA* **97**, 13384–13389 (2000).
- Ohta, H. *et al.* Ki16425, a subtype-selective antagonist for EDG-family lysophosphatidic acid receptors. *Mol. Pharmacol.* **64**, 994–1005 (2003).
- Heise, C.E. *et al.* Activity of 2-substituted lysophosphatidic acid (LPA) analogs at LPA receptors: discovery of a LPA1/LPA3 receptor antagonist. *Mol. Pharmacol.* **60**, 1173–1180 (2001).
- Strutz, F. *et al.* Identification and characterization of a fibroblast marker: FSP1. *J. Cell Biol.* **130**, 393–405 (1995).
- Lawson, W.E. *et al.* Characterization of Fibroblast Specific Protein 1 in Pulmonary Fibrosis. *Am. J. Respir. Crit. Care Med.* **171**, 899–907 (2005).
- Bucala, R., Spiegel, L.A., Chesney, J., Hogan, M. & Cerami, A. Circulating fibrocytes define a new leukocyte subpopulation that mediates tissue repair. *Mol. Med.* **1**, 71–81 (1994).
- Moore, B.B. *et al.* CCR2-mediated recruitment of fibrocytes to the alveolar space after fibrotic injury. *Am. J. Pathol.* **166**, 675–684 (2005).
- Zhang, K., Rekhter, M.D., Gordon, D. & Phan, S.H. Myofibroblasts and their role in lung collagen gene expression during pulmonary fibrosis. A combined immunohistochemical and in situ hybridization study. *Am. J. Pathol.* **145**, 114–125 (1994).
- Zhou, D. *et al.* Phosphatidic acid and lysophosphatidic acid induce haptotactic migration of human monocytes. *J. Biol. Chem.* **270**, 25549–25556 (1995).
- Goetzl, E.J., Kong, Y. & Voice, J.K. Cutting edge: differential constitutive expression of functional receptors for lysophosphatidic acid by human blood lymphocytes. *J. Immunol.* **164**, 4996–4999 (2000).
- Picker, L.J. *et al.* Differential expression of homing-associated adhesion molecules by T cell subsets in man. *J. Immunol.* **145**, 3247–3255 (1990).
- Hara, T., Jung, L.K., Bjorn Dahl, J.M. & Fu, S.M. Human T cell activation. III. Rapid induction of a phosphorylated 28 kD/32 kD disulfide-linked early activation antigen (EA 1) by 12-o-tetradecanoyl phorbol-13-acetate, mitogens, and antigens. *J. Exp. Med.* **164**, 1988–2005 (1986).
- Maino, V.C., Suni, M.A. & Ruitenberg, J.J. Rapid flow cytometric method for measuring lymphocyte subset activation. *Cytometry* **20**, 127–133 (1995).
- Fireman, E. *et al.* Morphological and biochemical properties of alveolar fibroblasts in interstitial lung diseases. *Lung* **179**, 105–117 (2001).
- Basset, F. *et al.* Intraluminal fibrosis in interstitial lung disorders. *Am. J. Pathol.* **122**, 443–461 (1986).
- Mills, G.B. & Moolenaar, W.H. The emerging role of lysophosphatidic acid in cancer. *Nat. Rev. Cancer* **3**, 582–591 (2003).
- Peng, X. *et al.* Protective effects of sphingosine 1-phosphate in murine endotoxin-induced inflammatory lung injury. *Am. J. Respir. Crit. Care Med.* **169**, 1245–1251 (2004).
- Chambers, R.C. & Laurent, G.J. Coagulation cascade proteases and tissue fibrosis. *Biochem. Soc. Trans.* **30**, 194–200 (2002).
- Kim, K.K. *et al.* Alveolar epithelial cell mesenchymal transition develops in vivo during pulmonary fibrosis and is regulated by the extracellular matrix. *Proc. Natl. Acad. Sci. USA* **103**, 13180–13185 (2006).
- Munger, J.S. *et al.* The integrin alpha v beta 6 binds and activates latent TGF beta 1: a mechanism for regulating pulmonary inflammation and fibrosis. *Cell* **96**, 319–328 (1999).
- Boucharaba, A. *et al.* Platelet-derived lysophosphatidic acid supports the progression of osteolytic bone metastases in breast cancer. *J. Clin. Invest.* **114**, 1714–1725 (2004).
- Honda, Y., Tsunematsu, K., Suzuki, A. & Akino, T. Changes in phospholipids in bronchoalveolar lavage fluid of patients with interstitial lung diseases. *Lung* **166**, 293–301 (1988).

43. Goetzl, E.J. *et al.* Gelsolin binding and cellular presentation of lysophosphatidic acid. *J. Biol. Chem.* **275**, 14573–14578 (2000).
44. Dinubile, M.J. Plasma gelsolin: in search of its raison d'etre. Focus on "Modifications of cellular responses to lysophosphatidic acid and platelet-activating factor by plasma gelsolin". *Am. J. Physiol. Cell Physiol.* **292**, C1240–C1242 (2007).
45. Allport, J.R. *et al.* Neutrophils from MMP-9- or neutrophil elastase-deficient mice show no defect in transendothelial migration under flow in vitro. *J. Leukoc. Biol.* **71**, 821–828 (2002).
46. Kim, N.D., Chou, R.C., Seung, E., Tager, A.M. & Luster, A.D. A unique requirement for the leukotriene B4 receptor BLT1 for neutrophil recruitment in inflammatory arthritis. *J. Exp. Med.* **203**, 829–835 (2006).
47. Xiao, Y.J. *et al.* Electrospray ionization mass spectrometry analysis of lysophospholipids in human ascitic fluids: comparison of the lysophospholipid contents in malignant vs nonmalignant ascitic fluids. *Anal. Biochem.* **290**, 302–313 (2001).
48. Means, T.K., Hayashi, F., Smith, K.D., Aderem, A. & Luster, A.D. The Toll-like receptor 5 stimulus bacterial flagellin induces maturation and chemokine production in human dendritic cells. *J. Immunol.* **170**, 5165–5175 (2003).
49. Reutershan, J. *et al.* Critical role of endothelial CXCR2 in LPS-induced neutrophil migration into the lung. *J. Clin. Invest.* **116**, 695–702 (2006).
50. Medoff, B.D. *et al.* BLT1-mediated T cell trafficking is critical for rejection and obliterative bronchiolitis after lung transplantation. *J. Exp. Med.* **202**, 97–110 (2005).